IET Biometrics 4.2 (2015): 42–52

DOI: http://dx.doi.org/10.1049/iet-bmt.2014.0087

Published in IET Biometrics
Received on 16th October 2014
Revised on 5th December 2014
Accepted on 5th January 2015
doi: 10.1049/iet-bmt.2014.0087

ISSN 2047-4938

Pre-registration of latent fingerprints based on orientation field

Ram Prasad Krish[1], Julian Fierrez[1], Daniel Ramos[1], Javier Ortega-Garcia[1], Josef Bigun[2]

[1]Biometric Recognition Group – ATVS, Escuela Politecnica Superior Universidad Autonoma de Madrid, Campus de Cantoblanco C/ Francisco Tomas y Valiente, 11 28049 Madrid, Spain
[2]Intelligent Systems Laboratory, Halmstad University, Box 823, Halmstad SE 30118, Sweden
E-mail: ram.krish@uam.es

Abstract: In this study, the authors present a hierarchical algorithm to register a partial fingerprint against a full fingerprint using only the orientation fields. In the first level, they shortlist possible locations for registering the partial fingerprint in the full fingerprint using a normalised correlation measure, taking various rotations into account. As a second level, on those candidate locations, they calculate three other similarity measures. They then perform score fusion for all the estimated similarity scores to locate the final registration. By registering a partial fingerprint against a full fingerprint, they can reduce the search space of the minutiae set in the full fingerprint, thereby improving the result of partial fingerprint identification, particularly for poor quality latent fingerprints. They report the rank identification improvements of two minutiae-based automated fingerprint identification systems on the National Institute of Standards and Technology (NIST)-Special Database 27 database when they use the authors hierarchical registration as a pre-alignment.

1 Introduction

Any impression made by the ridges in the skin of the human finger is generally termed as 'fingerprint'. Fingerprints which are revealed using some chemical or optical processing from a crime scene are called 'latent fingerprints'. These are unintentionally left fingerprints found in the crime scenes. In the realm of forensic analysis ('criminology'), the use of latent fingerprints is a routine procedure to identify suspects. Such practice has been followed for over a century now, and has most of the time proven to be pertinent in identifying the suspects. Consequently, the identity of an individual established on the basis of fingerprints is accepted by law enforcement agencies [1, 2].

Fingerprints are also widely used in civilian biometric recognition applications such as authentication, passport controls, biometric-based digital identity etc. Since the fingerprint is one of the oldest biometric traits, many techniques have been proposed in the literature for fingerprint recognition. It is comparatively a mature biometric trait compared against face, iris, voice etc. Automated fingerprint identification systems (AFIS) are widely used for fingerprint recognition in both forensic as well as commercial domains. Most AFIS currently use two prominent ridge characteristics (called 'minutiae') namely ridge-endings and bifurcations to compare fingerprints. The minutia-based decision is accepted as a proof of identity legally by courts in almost all countries around the world [1, 2].

In general, depending on the nature of the feature used by matching algorithms, fingerprint matching can be broadly classified into 'correlation-based matching, minutiae-based matching and non-minutiae feature-based matching'. In correlation-based matching, grey-scale fingerprint images of both input and reference are superimposed and pixel correlations are computed between them. In minutiae-based matching, minutiae stored as sets of points are compared using point pattern matching algorithms. In non-minutiae feature-based matching, other features of fingerprints such as orientation fields (OF), frequency maps, ridge shapes, texture information etc., are used for matching the input and the reference [2].

Irrespective of the core methodology used for fingerprint matching, the alignment between the input and the reference fingerprint is a crucial step. This is because the fingerprint images captured in different instances might have different rotation, translation or non-linear deformation between them. The main objective of fingerprint alignment is to estimate the transformation parameters between input and reference fingerprints.

The most widely used alignment method is based on minutiae. The main idea behind minutiae-based alignment is to search in the space of transformation parameters to find an optimal transformation with the maximum number of matched minutiae between the input and the reference. One such methodology is based on the generalised Hough transform (GHT) [3]. The main disadvantage for such technique is the inaccuracy in the transformation estimation because of discretisation of the parameters space. Other approaches could be to use brute force to check for all possible correspondences between minutiae pairs. There exist some alignment techniques that augment

minutiae with other supplementary features such as ridge information, OFs around a small neighbourhood of minutiae, geometric relationships between minutiae and its neighbours etc.

Alignment of full fingerprints is a well-studied problem. However, these methods are limited in alignment accuracy because of quantisation of transformation parameters, or are not adapted for the partial fingerprint scenario. Partial fingerprints can arise in a number of situations, for example [4, 5]: latent fingerprints lifted from crime scenes, because of small size of the fingerprint capturing devices, or an already enrolled fingerprint has noisy regions and is left only with a partial good/recognisable region for identification. The performance of the existing partial fingerprint identification systems mainly depends on the image quality, the number of minutiae available and other derived and extended features that can be obtained from the partial fingerprint region. Various approaches in partial fingerprint identification [5] include: the use of localised secondary features derived from relative minutia information [4], using representative points along ridge lines in addition to minutiae [6] and use of Level-3 features such as dots and incipients [7].

Most fingerprint matching algorithms, in general, assume approximately the same size of the minutiae set between the query and the reference minutiae for good identification accuracy [4]. It is nevertheless frequent in some scenarios to have very different sizes between query and reference because of the situations discussed above. Trying to align a partial fingerprint to a full fingerprint only based on minutiae features could lead to errors. Law enforcement agencies employ AFIS to shortlist the suspects from its criminal database (exemplar/tenprint fingerprints). In such a scenario, it is crucial that the performance accuracy of AFIS is as good as possible. Latent fingerprints inherently are of poor quality, which leads to poor identification accuracy of AFIS in the latent scenario as compared with full fingerprint identification.

To evaluate the performance of feature extraction and matching techniques of commercial AFIS, NIST has conducted a multi-phase open project called evaluation of latent fingerprint technologies (ELFT) [8]. In Phase-I of ELFT, the best performing system reported a Rank-1 identification accuracy of 80% in which 100 latents were compared against 10 000 rolled prints [9]. In Phase-II, Evaluation-1, the best performing system reported a Rank-1 identification accuracy of 97.2% in which 835 latents were compared against 100 000 rolled prints [10], and in Phase-II, Evaluation-2, the best performing system reported a Rank-1 identification accuracy of only 63.4% in which 1114 latents were compared against 100 000 rolled prints [11]. The reported accuracies from Phase-I and Phase-II cannot be directly compared as the database and the quality of the latents were different. In [12], it is concluded that only a limited class of latents benefits from automated procedures, but the procedures of marking the minutiae, determining the subjective quality of latents etc. still need to be carried out manually.

In this paper, we focus on the problem of aligning a partial fingerprint against a full fingerprint, especially of poor quality latents. Instead of minutiae, we used OFs to perform the alignment. We reduce fingerprint images to orientation images, and we look at the alignment problem as registering the partial fingerprint orientation image into the full fingerprint orientation image. Image registration is the process of overlaying (geometrically align) images of the same scene acquired in different times, different viewpoints and from different sensors [13].

Image registration is broadly classified into area-based and feature-based registration. We used area-based registration in our paper. The OF representing the flow of ridges is a relatively stable global feature of fingerprint images, and it represents the intrinsic nature of the fingerprint. The representative OF of a fingerprint is very less affected by the type of capture device, contrast variations and other quality effects compared with the input image or the minutiae. To improve the rank identification accuracy of minutiae-based matching, we consider only the minutiae around the region where the partial fingerprint orientation image is registered in the full fingerprint. This thereby reduces the search space of minutiae in the full fingerprint to approximately the size of partial fingerprint minutiae set, and consequently improves the performance of the minutiae-based matcher. A preliminary version of this work [14, 15] used correlation-based registration. Here, we extend that work by incorporating a hierarchical registration method.

The main contributions of this work are as follows:

1. New correlation-based hierarchical registration method for orientation images to register a partial fingerprint in a full fingerprint.
2. Experimental exploration of various types of OF generation methods adequate for the registration.
3. Experimental demonstration of the performance improvement of minutiae-based matching by incorporating our registration algorithm to reduce the search space of minutiae in full fingerprints. In particular, our algorithm significantly improves the rank identification accuracy for poor quality latents (bad and ugly categories) of NIST-Special Database 27 (SD27) database using NIST-Bozorth3 and Minutia Cylinder-Code (MCC)-software development kit (SDK) minutiae-based matchers.

In the following sections, we review related works on fingerprint OF-based registration, describe the database used in our experiments, the similarity measures used in our algorithm, followed by a detailed description of the proposed algorithm, experiments, results and conclusion.

2 Related works

2.1 OF-based registration

In this section, we review the OF-based fingerprint registration techniques in the literature, and its applicability in registering partial fingerprint images. A basic implementation of orientation-image registration requires computing the similarity between the input orientation image and the reference orientation image for every possible transformation considered between them (e.g. rotation and translation) [2]. Table 1 summarises various techniques in the literature for OF-based fingerprint registration together with their limitations for partial fingerprint registration.

Liu *et al.* [16] uses normalised mutual information (NMI) as the similarity measure between orientation images to perform fingerprint registration. They align fingerprint images by maximising NMI between the input and reference orientation images under different transformations. This technique is not suitable in aligning a partial fingerprint against full fingerprint as reported in [16]. In this

doi: 10.1049/iet-bmt.2014.0087

Table 1 Summary of OF-based fingerprint registration techniques in the literature together with their limitations to be applied for partial fingerprint registration

Method	Core technique	Limitations to partial fingerprint registration/ latent scenario
Liu *et al.* [16]	maximise the NMI between input and reference OF images	i) needs large area overlaps ii) more reference sample required to correctly estimate OF distribution
Nilsson and Bigun [17]	i) SP detection	i) SP not guaranteed in partial or latent fingerprints
	ii) 1D radiograms	ii) quantised projection angles, and require large area overlaps
Yager and Amin [18, 19]	i) DLO ii) generalised Hough transform iii) SD	i) SP not guaranteed in partial or latent fingerprints ii) needs large area overlaps

approach, for good alignment, the size of input and reference orientation images should be almost of similar size. Another drawback in this technique is the necessity of enough samples of reference fingerprints to correctly estimate the distribution of the OF, otherwise it leads to incorrect alignment. Both of these scenarios are not pertinent in forensic fingerprint identification.

Nilsson and Bigun [17] focus on registering the fingerprints by complex filtering and by one-dimensional (1D) projections of orientation images. Given the orientation images of the fingerprints represented as complex OFs, they first use specific complex filters to locate singular points (SPs) (core and delta) in the fingerprint. Once these SPs are located in both input and reference orientation images, transformation parameters (rotation and translation) are estimated by superimposing the SPs. Another technique studied in [17] is 1D projections of orientation images. In this method, the fingerprint image is decomposed into six equally spaced directions called orientation images, and a Radon transformation is used to compute 1D projections of these orientation images (called radiograms). A translation parameter is estimated between a pair of radiograms from input and reference belonging to the same projection angle by a correlation measure. When utilising this method, it is already assumed that the rotation alignment between input and reference is negligible or is already corrected. These techniques cannot be adapted to register partial fingerprints because SPs are not always guaranteed in partial fingerprint, and the area of overlap between input and reference is often small.

Yager and Amin [18, 19] explore three types of OF registration techniques summarised as follows:

1. *Distinctive local orientations (DLO):* This approach mainly depends on distinctive patterns in the OF called SPs (core and delta). This is similar to the work in [17], except for the technique to locate the SPs.
2. *GHT:* In this approach, the space of all possible transformation parameters is discretised and analysed for the best transformation.
3. *Steepest descent (SD):* Starting with some initial parameters, this algorithm evaluates a cost function. It then evaluates a sample of local neighbourhood in the parameter space and selects the parameters that give greatest descent in the cost. This procedure is repeated until a local minimum has been found.

It is reported in [18] that both GHT and SD do not perform well when the area of overlap between the input and reference is small, similar to the case using NMI [16]. Therefore both GHT and SD are not suitable for partial fingerprint registration. Moreover, DLO looks for SPs, and it is not assured that a partial fingerprint will have SP in it. Therefore all the OF registration techniques proposed in the literature are not suitable for partial fingerprint registration, and cannot be quickly adapted to this scenario.

2.2 Other registration techniques

There are two main approaches in pre-alignment, namely: 'absolute pre-alignment' and 'relative pre-alignment' [2]. The OF-based registration in this work falls under the category of relative pre-alignment.

In 'absolute pre-alignment', the reference fingerprints are pre-aligned independently of the input fingerprint before storing in the database. The input fingerprint is pre-aligned just once before any comparisons are performed with the reference fingerprints. For absolute pre-alignment, the most common technique is to translate the fingerprint according to position of the core point. There are also other techniques which focus on absolute pre-alignment based on the shape of the external fingerprint silhouette, orientation of delta or core points or average orientations in the neighbourhood of cores. Since all these absolute pre-alignment depends on the SPs, and for latent fingerprints SPs are not guaranteed, absolute pre-alignment is not possible for latent scenario.

In 'relative pre-alignment', the input fingerprint has to be pre-aligned with respect to the reference fingerprints while matching. The most common techniques in relative pre-alignment are performed by superimposing the SPs (core or delta), by comparing ridge features or by correlating the orientation images. Superimposing SPs are not feasible in latent scenario as they are not always guaranteed in latent fingerprint images. The ridge features, that is, length and orientation of the ridge on which a minutiae resides, seem to be possible feature candidate, but a reliable extraction of ridge features from bad or ugly quality latent fingerprints is a challenging problem. Estimation of OF is more reliable as compared against ridge feature extraction in latent fingerprints. Therefore we used the method of correlating the orientation images in this paper to register a partial fingerprint in a full fingerprint.

3 Database

NIST-SD27 [20] is a publicly available forensic fingerprint database which comprises of 258 latent fingerprint images, its matching tenprint images and their minutiae sets. The NIST-SD27 minutia set database is classified into two [20, 21]: (i) 'ideal' and (ii) 'matched' minutiae sets. The 'ideal' minutiae set for latents was manually extracted by a forensic examiner without any prior knowledge of its corresponding tenprint image. The 'ideal' minutiae set for tenprints was initially extracted using an AFIS, and then these minutiae were manually validated by at least two forensic examiners. The 'matched' minutiae set contains

those minutiae which are in common between the latent and its mated tenprint image. There is a one-to-one correspondence in the minutiae between the latent and its mate in the matched minutia set. This ground truth (matched minutiae set) was established manually by a forensic examiner looking at the images and the 'ideal' minutiae.

The NIST-SD27 database consists of latent fingerprint images of varying quality. Each image is of 800×768 pixels in size and has been scanned at 500 pixels per inch as a grey-scale image. It already contains a classification of the latent fingerprints based on the subjective quality of the image into good, bad and ugly, containing 88, 85 and 85 fingerprints, respectively, determined by the forensic examiner. The average number of minutiae for good, bad and ugly category latents are 32, 18 and 12, respectively. Fig. 1 shows sample images from the NIST-SD27 database which belong to good, bad and ugly quality categories, respectively. In [22], it is shown that there is a correlation between this subjective quality classification and the matching performance.

4 Similarity measures

In this section, we introduce various similarity measures that are used in our hierarchical registration algorithm.

Let $\boldsymbol{U}$ and $\boldsymbol{V}$ be discrete images of the same size, represented as a 2D array where the array elements may represent values of grey pixels ('zero-order tensors'), colour pixels ('first-order tensors') or local directions ('second-order tensors').

The Schwarz inequality

$$\frac{|\langle \boldsymbol{U},\ \boldsymbol{V}\rangle|}{\|\boldsymbol{U}\| \times \|\boldsymbol{V}\|} \leq 1 \tag{1}$$

holds for $\boldsymbol{U}$ and $\boldsymbol{V}$ [23, Chapter 3]. Here, $\langle \boldsymbol{U}, \boldsymbol{V}\rangle$ is the inner product between $\boldsymbol{U}$ and $\boldsymbol{V}$ calculated as

$$\langle \boldsymbol{U},\ \boldsymbol{V}\rangle = \sum_{r,c} \boldsymbol{U}(r,\ c)^* \cdot \boldsymbol{V}(r,\ c) \tag{2}$$

where r, c are the indices, $\boldsymbol{U}(r, c)$* is the complex conjugate of $\boldsymbol{U}(r,\ c)$, and $\|\boldsymbol{U}\|$ and $\|V\|$ are the L_2 norms of $\boldsymbol{U}$ and $\boldsymbol{V}$, respectively.

The L_2 norm $\|\boldsymbol{U}\|$ is calculated as

$$\|\boldsymbol{U}\| = \left[\sum_{r,c} \boldsymbol{U}(r,\ c)^* \cdot \boldsymbol{U}(r,\ c)\right]^{1/2} \tag{3}$$

and similarly for $\|\boldsymbol{V}\|$.

The normalised correlation between $\boldsymbol{U}$ and $\boldsymbol{V}$, referred to as Schwarz Similarity (SS) hereafter is defined as

$$\mathrm{SS}(\boldsymbol{U},\ \boldsymbol{V}) = \frac{|\langle \boldsymbol{U},\ \boldsymbol{V}\rangle|}{\|\boldsymbol{U}\| \times \|\boldsymbol{V}\|} \tag{4}$$

Owing to (1), the interval for SS($\boldsymbol{U}$, $\boldsymbol{V}$) is in the range [0, 1]. By calculating SS as a similarity measure, we can locate a given pattern (a small image) in a large image. When SS($\boldsymbol{U}$, $\boldsymbol{V}$) is 1, then both $\boldsymbol{U}$ and $\boldsymbol{V}$ are viewed as most similar patterns, and when SS($\boldsymbol{U}$, $\boldsymbol{V}$) is 0, they are least similar [23].

Assuming $\boldsymbol{U}$ and $\boldsymbol{V}$ represent local directions ('second-order tensors') in the range [−90°, +90°), we define the Manhattan-based Similarity MS($\boldsymbol{U}$, $\boldsymbol{V}$) as

$$\mathrm{MS}(\boldsymbol{U},\ \boldsymbol{V}) = \cos\left(\frac{1}{N}\sum_{r,c}\left(\Delta_{r,c}^{U,V}\right)\right) \tag{5}$$

and Euclidean-based similarity ES($\boldsymbol{U}$, $\boldsymbol{V}$) as

$$ES(\boldsymbol{U},\ \boldsymbol{V}) = \cos\left(\left[\frac{1}{N}\sum_{r,c}\left(\Delta_{r,c}^{U,V}\right)^2\right]^{1/2}\right) \tag{6}$$

where

$$\Delta_{r,c}^{U,V} = \min\left(|\boldsymbol{U}(r,\ c) - \boldsymbol{V}(r,\ c)|,\quad 180 - |\boldsymbol{U}(r,\ c) - \boldsymbol{V}(r,\ c)|\right) \tag{7}$$

which takes values in the range [0, +90°) and N is the size in pixels of $\boldsymbol{U}$ or $\boldsymbol{V}$ ($\boldsymbol{U}$ and $\boldsymbol{V}$ are of same size). Owing to (7), the value of MS and ES will be in the range [0, 1].

The Consistency Similarity CS($\boldsymbol{U}$, $\boldsymbol{V}$) (which was proposed in [24]) is defined as

$$CS(\boldsymbol{U},\ \boldsymbol{V}) = \frac{1}{N}\left|\sum_{r,c} \mathrm{e}^{i2\left(\boldsymbol{U}(r,c) - \boldsymbol{V}(r,c)\right)}\right| \tag{8}$$

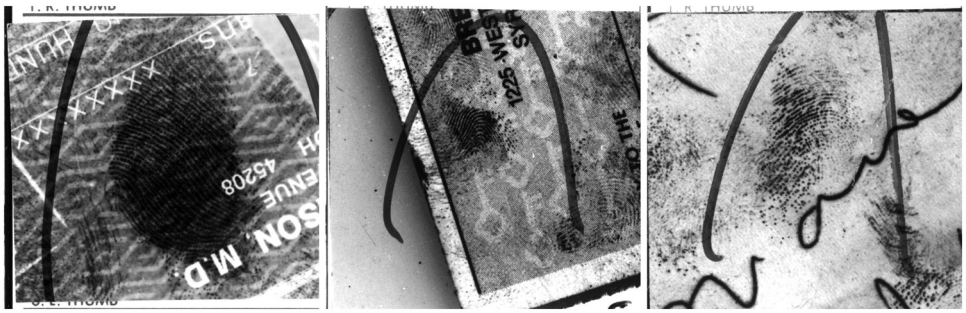

a *b* *c*

Fig. 1 *Subjective quality classification of latent fingerprint images in NIST-SD27 database*

a Good
b Bad
c Ugly

doi: 10.1049/iet-bmt.2014.0087

where i is the complex number $\sqrt{-1}$ and $|z|$ is the magnitude of complex number z. The CS averages the unit vector whose phase is doubled orientation difference, and the value is in the range [0, 1].

All the similarity measures SS, MS, ES and CS are in the normalised range [0, 1] and these measures can be fused directly.

5 Algorithm

The algorithm to register the OF of the latent fingerprint with that of the tenprint fingerprint is achieved in two hierarchical levels. In the first level, we perform the normalised correlation between the OF of latent and tenprint for various rotation alignments in the range [−45°, +45°] with 1° increments. We then shortlist the correlation peaks for each rotation. These peaks are the possible target locations for registration.

We observed that deciding the target location only based on the normalised correlation score does not always yield satisfactory results. Therefore, a second level, on these candidate locations, we calculate MS, ES and CS similarity measures between the latent centred at the peak location in the tenprint. The final registration location is chosen from the candidate locations as the one that maximises the mean similarity between SS, MS, ES and CS. This gives better registration accuracies than deciding only based on SS. In the following section, we describe this approach in more detail.

5.1 Level 1: normalised correlation

Step 1: Generate the OF L for the latent fingerprint and T for the tenprint fingerprint as detailed in Section 6. The orientations are obtained for 16×16 block sizes, and are in the range [−90°, +90°). Figs. 2*a* and *b* shows the OF reconstructed from the minutiae set of latent and tenprint, respectively. The expected outcome of the registration algorithm is to locate the minutiae region shown in Fig. 2*c*.
Step 2: Generate the orientation tensors $\bar{L}$ and $\bar{T}$ for the latent L and tenprint T, respectively, in double angles (i.e. in the range [−180, +180]°) using complex numbers, as follows

$$\begin{aligned} \bar{L} &= \exp(i \times 2 \times \theta_{\mathrm{L}}) \\ \bar{T} &= \exp(i \times 2 \times \theta_{\mathrm{T}}) \end{aligned} \tag{9}$$

where i is the complex number $\sqrt{-1}$, θ_{L} and θ_{T} are the angles of L and T from step 1. $\bar{L}$ is the smallest rectangular region that covers the latent minutiae.

For each subregion $\bar{T}_{\mathrm{s}}$ of $\bar{T}$ that is of the same size as $\bar{L}$ located at a position indexed by s, we can find the inner product between $\bar{L}$ and $\bar{T}_{\mathrm{s}}$ as follows

$$\langle \bar{L},\ \bar{T}_{\mathrm{s}} \rangle = \sum_{r,c} \bar{L}(r,\ c)^* \cdot \bar{T}_{\mathrm{s}}(r,\ c) \tag{10}$$

where r, c are the indices, $\bar{L}(r,\ c)^*$ is the complex conjugate of $\bar{L}(r,\ c)$.
Step 3: Define the bounding box for the latent orientation tensors $\bar{L}$ by discarding the background. The bounding box can be estimated by the minimum and maximum row and column numbers that correspond to the foreground of latent orientation tensors.
Step 4: When searching for the pattern $\bar{L}$ in $\bar{T}$, it is possible that $\bar{L}$ is not perfectly aligned with $\bar{T}$, rotation wise. To compensate for the rotation alignment, we need to test the latent $\bar{L}$ against tenprint $\bar{T}$ for various rotations of $\bar{L}$. In our experiments, we rotate $\bar{L}$ in the range [−45°, +45°] with a step size $\Delta\theta$ of 1° to compensate for rotation alignment to generate $\bar{L}^{\theta}$. A geometric rotation of $\Delta\theta$ implies a related rotation of the tensor field of $2\Delta\theta$.
Step 5: The correlation is obtained by generating $\langle \bar{L}^{\theta}, \bar{T}_{\mathrm{s}} \rangle$ for all locations s in $\bar{T}$. The result of this operation is a complex image. We then observe the correlation peaks for all θ (magnitude of the complex image). Figs. 2*d–f* show the magnitude of the correlation images of $\bar{L}^{-35^{\circ}}$, $\bar{L}^{+1^{\circ}}$ and $\bar{L}^{+35^{\circ}}$ with $\bar{T}$, respectively.
Step 6: For each θ from the correlated result, find the location of the peak $s^{\theta} = (r_m^{\theta},\ c_m^{\theta})$, that is, the location with maximum magnitude in the correlated image. The peak in the correlated image is where $\bar{L}^{\theta}$ agrees the most in $\bar{T}$. $S = \{(r_m^{\theta},\ c_m^{\theta})\}$ is the set containing the coordinates of the correlation peaks for all θ.
Step 7: For all orientations θ, calculate $\mathrm{SS}(\bar{L}^{\theta},\ \bar{T}_{\mathrm{s}}^{m})$, where $\bar{T}_{\mathrm{s}}^{m}$ is the subregion in $\bar{T}$ whose centre is $s^{\theta} = (r_m^{\theta},\ c_m^{\theta})$. SS is the normalised correlation measure as defined in (4).

The correlation and normalised correlation are essentially equivalent in the scenario where θ_{L} and θ_{T} are not estimated from grey pixel gradients, but reconstructed from minutiae orientations. Consequently, the orientation tensors $e^{i2\theta_{\mathrm{L}}}$ and $e^{i2\theta_{\mathrm{T}}}$ are complex numbers falling on a unit circle. Therefore the magnitude of the orientation tensors thus obtained is always 1.

5.2 Level 2: fusion of similarity scores

Step 8: For each $s^{\theta} = (r_m^{\theta},\ c_m^{\theta}) \in S$, calculate $\mathrm{MS}(\bar{L}^{\theta},\ \bar{T}_{\mathrm{s}}^{m})$, $\mathrm{ES}(\bar{L}^{\theta},\ \bar{T}_{\mathrm{s}}^{m})$ and $\mathrm{CS}(\bar{L}^{\theta},\ \bar{T}_{s^m})$ as defined in (5), (6) and (8), respectively.
Step 9: SS, MS, ES and CS are all similarity scores in the range [0, 1], where 0 denotes minimum similarity and 1 denotes maximum similarity. We perform score fusion of SS, MS, ES and CS based on the mean rule, and look for the $s^{\theta} = (r_m^{\theta},\ c_m^{\theta}) \in S$ for which the fused similarity score is maximum.
Step 10: The resulting $(r_m^{\theta},\ c_m^{\theta})$ is the location in the tenprint where the latent rotated at θ is registered with best alignment (see Fig. 2*g*). The centre of the latent L is registered to $(r_m^{\theta},\ c_m^{\theta})$ in tenprint T, and with a radius half the diagonal length of the bounding box of the latent OF, a subset of minutiae which falls inside this circular region is chosen (see Fig. 2*h*).

6 Types of OF estimation techniques

In this paper, we have used five different techniques for computing the OF of the fingerprints:

1. Manually estimated OF from the fingerprint image [25] ('MANUAL_OF').
2. OF estimated directly from fingerprint image using local Fourier analysis [26], and then performing context-based correction of the OF using dictionary lookup of orientation patches [25] ('DICT_OF').
3. OF estimated directly from the fingerprint image using gradient-based approach [27] ('IMG_OF').
4. OF reconstructed from the minutiae [28] ('MINU_OF').
5. OF estimated by taking the average of both of 'IMG_OF' and 'MINU_OF', denoted as 'AVG_OF'.

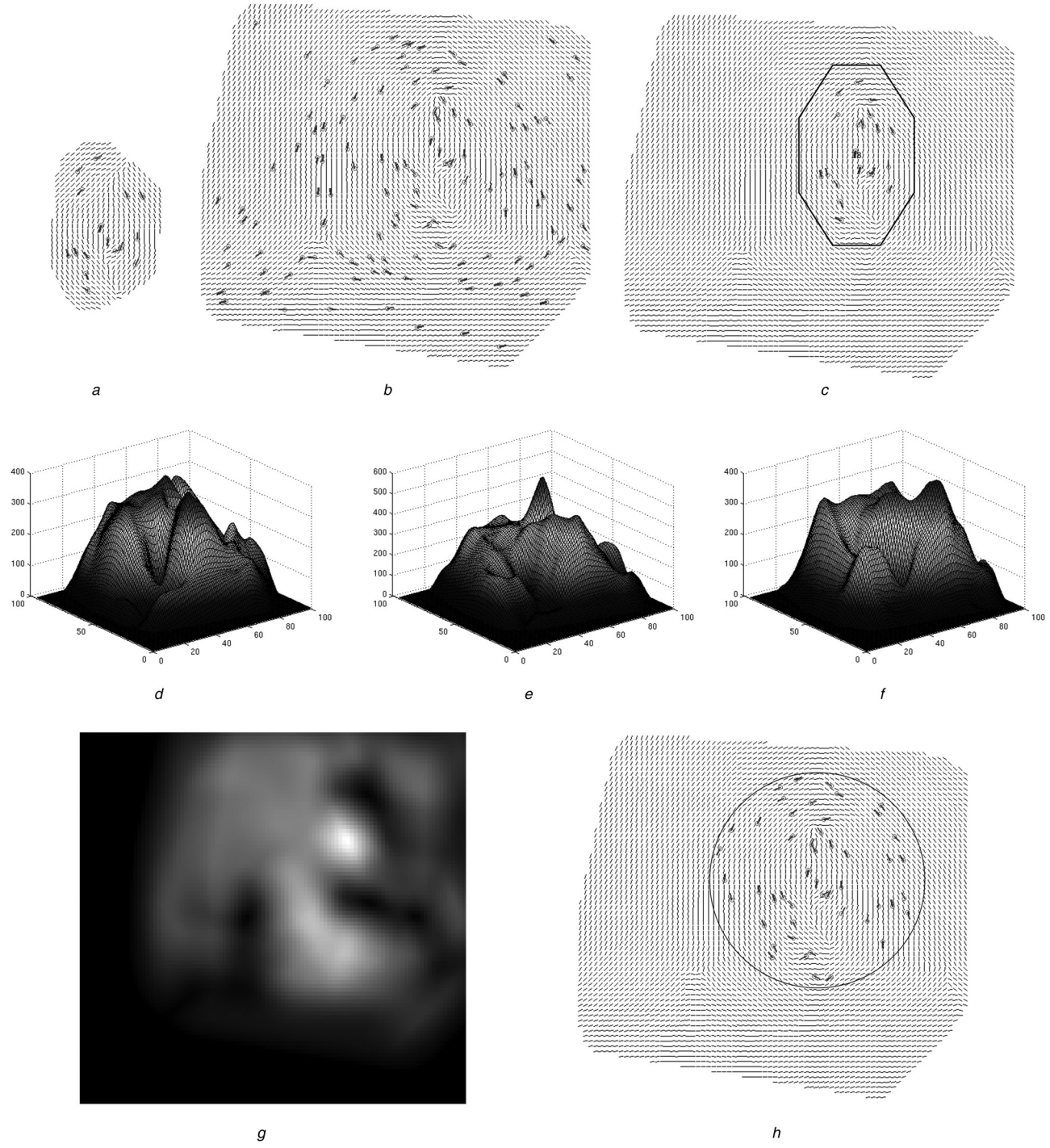

Fig. 2 *Various stages in the registration algorithm shown on G028L1 (latent) and G028T1 (tenprint) of NIST-SD27*

a, b OF reconstructed from the ideal minutiae set, with the minutiae plotted over the OF
c Region in the tenprint that is to be found after registration of (*a*) into (*b*). (*d*)–(*f*) are the correlation peaks when the latent is rotated at −35°, 1° and +35°, respectively, and correlated with tenprint
g Region where the latent pattern is identified in the tenprint based on the proposed score fusion for rotation alignment of +1°
h Minutiae region selected by our pre-alignment algorithm

'AVG_OF' is estimated using the technique proposed in [29], also detailed in [2, Chapter 3] to average local gradients.

Let θ_k^i and θ_k^m be the orientation corresponding to kth block of 'IMG_OF' and 'MINU_OF', respectively. We double the angles to encode them by vectors

$$\bar{\boldsymbol{d}}_k^i = [\cos(2\theta_k^i), \quad \sin(2\theta_k^i)] \tag{11}$$

$$\bar{\boldsymbol{d}}_k^m = [\cos(2\theta_k^m), \quad \sin(2\theta_k^m)] \tag{12}$$

where $\bar{\boldsymbol{d}}_k^i$ and $\bar{\boldsymbol{d}}_k^m$ are the vectors corresponding to θ_k^i and θ_k^m.

We then find the average vector $\bar{\boldsymbol{d}}_k^a = [\text{avg}\cos_k^a, \ \text{avg}\sin_k^a]$ where

$$\text{avg}\cos_k^a = 0.5 \times (\cos(2\theta_k^i) + \cos(2\theta_k^m)) \tag{13}$$

$$\text{avg}\sin_k^a = 0.5 \times (\sin(2\theta_k^i) + \sin(2\theta_k^m)) \tag{14}$$

From this average vector $\bar{\boldsymbol{d}}_k^a$, find the corresponding

doi: 10.1049/iet-bmt.2014.0087

orientation of the kth block of 'AVG_OF' as

$$\theta_k^a = 0.5 \times a\tan2(\text{avg } \sin_k^a,\ \text{avg } \cos_k^a) \quad (15)$$

The double angle representation avoids any errors because of circularity of angles while averaging. Here, we assume θ_k^i, θ_k^m and θ_k^a are in radians.

Out of these five different techniques, 'MANUAL_OF' and 'DICT_OF' were used for latent fingerprints, whereas 'DICT_OF, IMG_OF, MINU_OF and AVG_OF' were used for tenprints. All the OF estimated were of 16×16 block size. The region of interest for the fingerprint is considered to be the region inside the convex hull of the corresponding ideal minutiae of the fingerprint present in NIST-SD27.

7 Experiments

We perform experiments on good, bad and ugly quality classifications of NIST-SD27 to report the accuracy of the proposed registration algorithm. About 88 latents of good category, 85 latents of bad category and 85 latents of ugly category were searched in the entire set of 258 tenprints in the NIST-SD27 database. We report the rank identification accuracy for two publicly available minutiae-based matchers, namely NIST-Bozorth3 [30] and MCC SDK [31–34] before and after incorporating our proposed hierarchical registration algorithm as a pre-registration before the identification.

When reporting the rank identification accuracies, for good quality, there are 88 match scores and 88×257 non-match scores, for bad and ugly qualities, there are 85 match scores and 85×257 non-match scores, respectively. When we report the rank identification accuracy for the entire NIST-SD27 database (all category), then there are 258 match scores and 258×257 non-match scores.

NIST-Bozorth3 is a minutiae-based fingerprint matcher that is specially developed to deal with latent fingerprints. This matcher is part of the NIST Biometric Image Software [30], developed by NIST. MCC-SDK is a well-known minutiae matcher more adapted to good quality fingerprints with reasonable number of minutiae in both query and reference templates. Both NIST-Bozorth3 and MCC-SDK are publicly available. We show the performance accuracy of the matcher using cumulative match characteristic (CMC) curves.

7.1 Experiment 1: choosing the best OF for tenprints

Fig. 3 shows the CMC curve of the NIST-Bozorth3 matcher when using 'MANUAL_OF' for latent against various other OF estimation techniques for tenprints while performing pre-registration using our proposed hierarchical method. We can observe that the rank identification accuracy has a consistent improvement when 'AVG_OF' is used for tenprints. The improvement while using 'AVG_OF' is mainly because the image noise introduced in the estimation of 'IMG_OF' is reduced while averaging with 'MINU_OF'.

On the basis of this result, we have chosen 'AVG_OF' as the OF for tenprints in remaining experiments reported here.

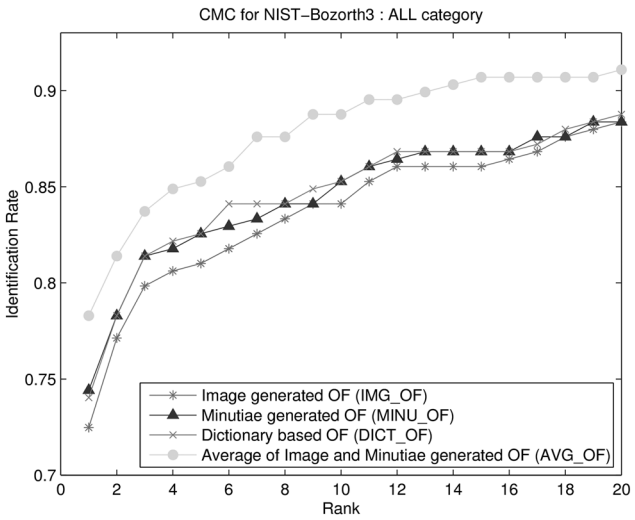

Fig. 3 *CMC curve showing the rank identification rate of NIST-Bozorth3 for NIST-SD27 when different types of OF estimation techniques were used for the tenprints, and MANUAL_OF for latents, when applying the proposed OF-based pre-alignment*

7.2 Experiment 2: pre-registration

In this experiment, we perform pre-registration using our registration algorithm to reduce the minutiae search space of the tenprint minutiae set, and then use the reduced minutiae set template as the reference template for the matcher. We used NIST-Bozorth3 and MCC-SDK as the minutiae-based matchers.

For latents, 'MANUAL_OF' and 'DICT_OF' were used, and for the tenprints we used 'AVG_OF' to report the rank identification accuracies in this experiment. We also analyse separately the performance of the matcher using correlation only based registration and using hierarchical registration.

7.2.1 NIST-Bozorth3: Figs. 4 and 5 show the CMC curve of NIST-Bozorth3 for two different registration levels when 'MANUAL_OF' and 'DICT_OF' are used for latents, respectively.

Fig. 4*a* shows the rank identification accuracy of NIST-Bozorth3 when correlation-based registration (Level 1) of our algorithm is used as pre-registration, and also without using pre-registration ('MANUAL_OF' for latents). We see a significant and consistent improvement in the rank identification accuracy for all the quality categories when incorporating the proposed pre-registration.

Fig. 4*b* shows the rank identification accuracy of NIST-Bozorth3 when hierarchical registration (Level 2) of our algorithm is used as pre-registration with 'MANUAL_OF' for latents. Here, we note a consistent improvement in the CMC curve for all subjective quality categories compared with the correlation-based registration. Especially, there is a significant improvement for both bad and ugly quality categories.

Table 2 summarises the Rank-1 identification accuracy of NIST-Bozorth3 for both correlation-based registration and hierarchical registration when 'MANUAL_OF' is used for latents. The column 'DIRECT' represents the Rank-1 identification accuracy of NIST-Bozorth3 when no pre-registration is applied to the minutiae set. Columns $L1$

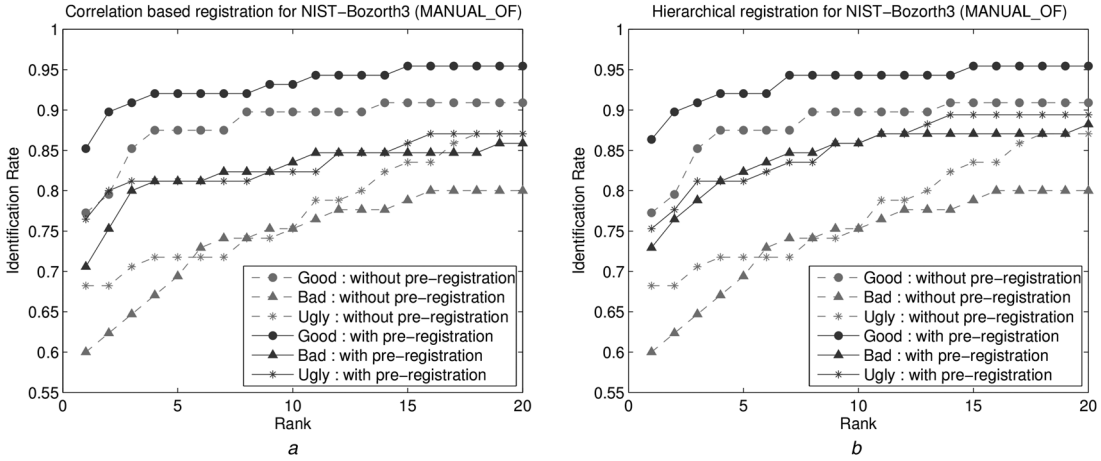

Fig. 4 *Performance of NIST-Bozorth3 when using MANUAL_OF for latents*

a Correlation only based registration (Level 1)
b Hierarchical registration (Level 2)

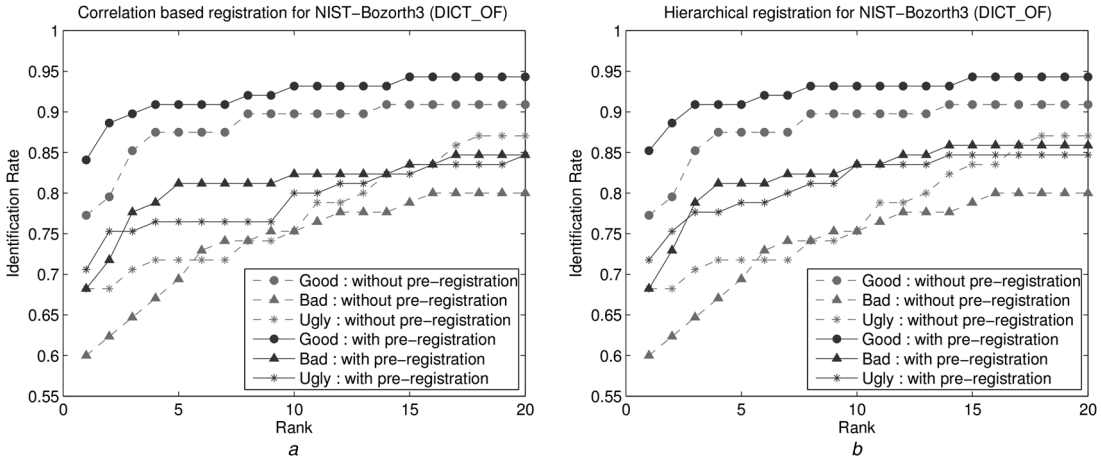

Fig. 5 *Performance of NIST-Bozorth3 when using DICT_OF for latents*

a Correlation only based registration (Level 1)
b Hierarchical registration (Level 2)

and *L*2 represent the Rank-1 identification accuracy for correlation-based registration (Level 1) and hierarchical based registration (Level 2), respectively.

Similarly, Figs. 5*a* and *b* shows the rank identification accuracy of NIST-Bozorth3 when correlation-based pre-registration and hierarchical pre-registration were applied using 'DICT_OF' for the latents. Table 3 summarises the Rank-1 identification accuracy in this case. Similar results compared with using 'MANUAL_OF' for the latents are also obtained here when considering 'DICT_OF'. This proves the robustness of the 'DICT_OF' method for obtaining a reliable OF even with very difficult latents and the feasibility of our method as a fully automatic tool.

7.2.2 MCC-SDK: Fig. 6 shows the CMC curve of MCC-SDK for the two registration levels considered when 'MANUAL_OF' is used for latents. Figs. 6*a* and *b* show the rank identification accuracy of MCC-SDK when correlation-based pre-registration and hierarchical pre-registration were applied, respectively. Table 4 summarises the Rank-1 identification accuracy in this case. The overall Rank-1 accuracy improved from 78.3 to 79.4% when incorporating Level 1 pre-registration, and to 79.4%

Table 2 Rank-1 identification for NIST-Bozorth3 with correlation-based pre-registration and hierarchical registration when 'MANUAL_OF' is used for latents

Quality	Bozorth3 DIRECT, %	Bozorth3 L1, %	Bozorth3 L2, %
all	68.6	77.52	78.29
good	77.27	85.23	86.36
bad	60.00	70.59	72.94
ugly	68.24	76.47	75.29

Table 3 Rank-1 identification for NIST-Bozorth3 with correlation-based pre-registration and hierarchical registration when 'DICT_OF' is used for latents

Quality	Bozorth3 DIRECT, %	Bozorth3 L1, %	Bozorth3 L2, %
all	68.6	74.42	75.19
good	77.27	84.09	85.23
bad	60.00	68.24	68.24
ugly	68.24	70.59	71.76

doi: 10.1049/iet-bmt.2014.0087

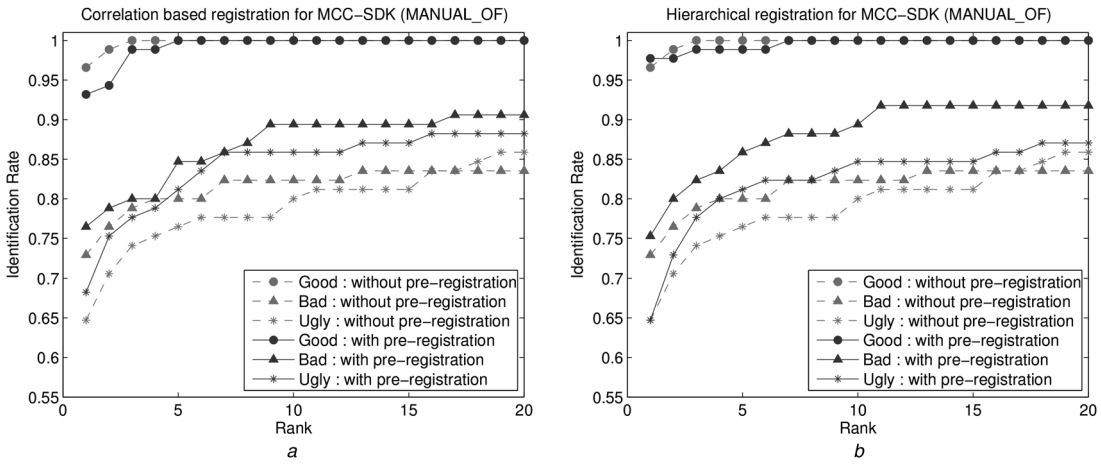

Fig. 6 *Performance of MCC-SDK when using MANUAL_OF for latents*

a Correlation only based registration (Level 1)
b Hierarchical registration (Level 2)

when hierarchical based pre-registration (Level 2) is incorporated. Even though the improvement is small, it is consistent and increases for bad and ugly quality categories when we look beyond Rank-1.

7.3 Experiment 3: parameters – rotation step size, radius

In this experiment, we study the quantisation step size for rotation alignment (step 4 in algorithm) as well as the best radius of the circular region (step 10 in algorithm) to generate the subset of minutiae from the tenprint minutiae set. We used 'MANUAL_OF' for the latents, 'AVG_OF' for tenprints and performed hierarchical registration on NIST-Bozorth3 matcher.

Table 4 Rank-1 identification for MCC-SDK with correlation-based pre-registration and hierarchical registration when 'MANUAL_OF' is used for latents

Quality	MCC-SDK DIRECT, %	MCC-SDK with L1, %	MCC-SDK L2, %
all	78.29	79.46	79.46
good	96.59	93.18	97.73
bad	72.94	76.47	75.29
ugly	64.71	68.24	64.71

From Fig. 7*a*, we can observe that when we use a step size (*X*-axis) for the rotation equal to 1°, we obtain the best performance in terms of rank identification accuracy (*Y*-axis). We looked at the Rank-5 identified accuracy of the NIST-SD27 database (all category) to evaluate the performance, and looked at the step size varying from 1° to 25°. Also interestingly, the performance is not very much degraded with large steps, which can justify the use of large steps in some scenarios when computation speed is prioritised.

With 1° as the step size, we studied the effect of the radius of the circular region. We observe that the optimal radius is obtained using a scale factor of 0.7 on half the length of the diagonal of bounding box. Fig. 7*b* shows the Rank-5 accuracy for various scales of the radius ranging from 0.6 to 1.4 scale factor in *X*-axis and the corresponding Rank-5 accuracy in *Y*-axis.

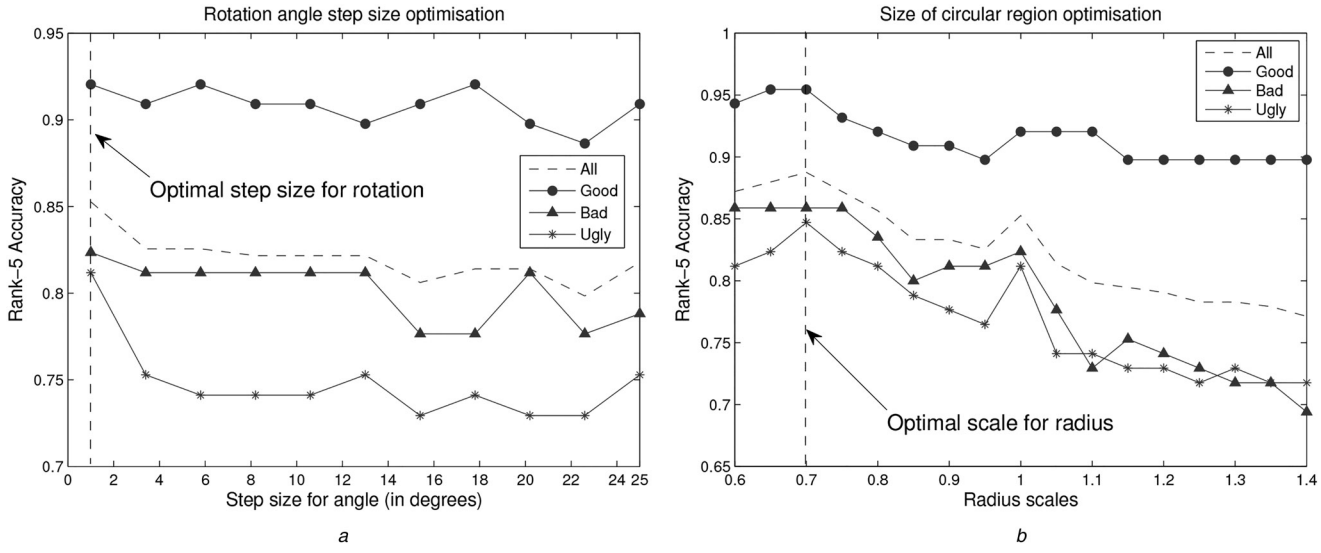

Fig. 7 *Finding the optimal value for rotation step size and radius scales using NIST-Bozorth3 matcher*

a Change in Rank-5 accuracies when increasing the step size in the range 1–25°
b Change in Rank-5 accuracies when changing the scale factor from 0.6 to 1.4

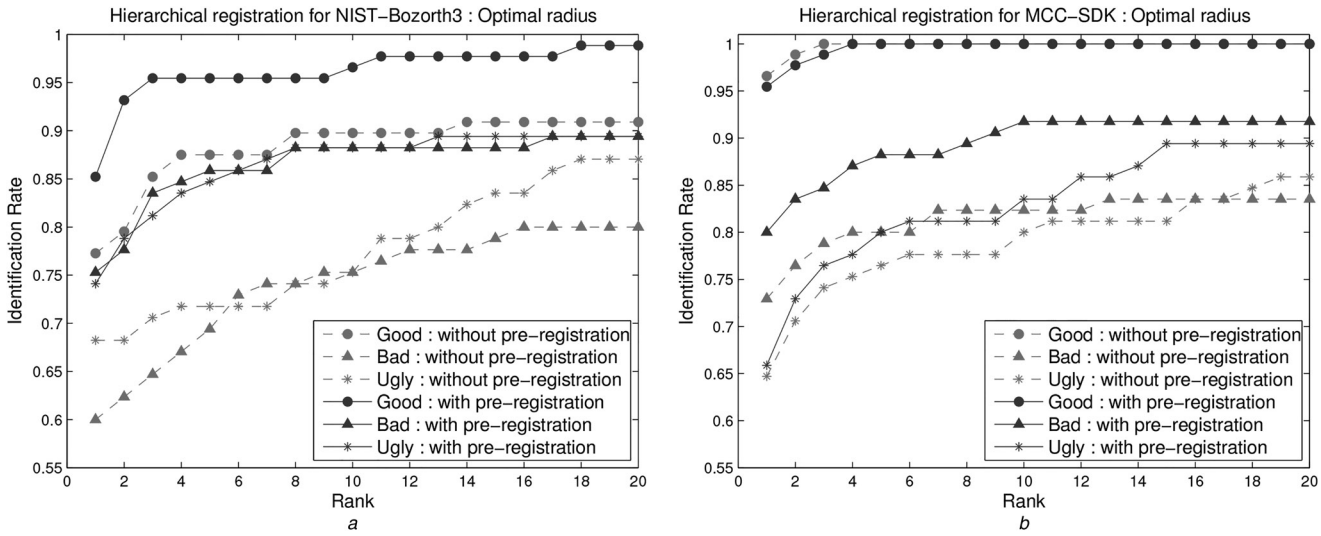

Fig. 8 *CMC curve of NIST-Bozorth3 and MCC-SDK with the optimal parameters*

a NIST-Bozorth3: hierarchical registration with optimal parameters
b MCC-SDK: hierarchical registration with optimal parameters

Table 5 Rank-1 identification for NIST-Bozorth3 and MCC-SDK with optimal parameters

Quality	NIST-Bozorth3 DIRECT, %	NIST-Bozorth3 with L2, %	MCC-SDK DIRECT, %	MCC-SDK with L2, %
all	68.6	78.29	78.29	80.62
good	77.27	85.23	96.59	95.45
bad	60.00	75.29	72.84	80.00
ugly	68.24	74.12	64.71	65.88

7.4 Experiment 4: best result obtained

With the optimal parameters estimated from our experiments, we have obtained the best performance boost for the matchers when using the hierarchical registration as a pre-registration. Figs. 8*a* and *b* show the CMC curve for both NIST-Bozorth3 and MCC-SDK with the optimal parameters for the hierarchical pre-registration. 'MANUAL_OF' was used for latents and 'AVG_OF' was used for tenprints. Table 5 summarises the Rank-1 identification accuracy of NIST-Bozorth3 and MCC-SDK for the optimal parameters (rotation step size with 1° and radius scale factor of 0.7).

Using our registration algorithm as a pre-registration, we were able to boost the overall Rank-1 identification accuracy from 68.60 to 78.29% for NIST-Bozorth3, and from 78.29 to 80.62% for MCC-SDK. In other regions of the CMC curve, the improvement is even higher.

7.5 Experiment 5: runtime analysis

We have implemented the proposed hierarchical registration algorithm in MATLAB which is not an optimised version to be directly compared with that of a corresponding C/C++ implementation. Nevertheless, we summarise the average runtime of the MATLAB version for each subjective quality category in Table 6.

Table 6 Average runtime for each subjective quality category

Quality	Average runtime in milliseconds, ms
good	921
bad	792
ugly	707

We assume that the minutiae extraction and computation of 'AVG_OF' are pre-computed offline, and they need to be generated only once for the reference fingerprints in the database.

In our MATLAB implementation, we used 'filter2()' function to obtain the correlations mentioned in step 5 of algorithm. If the size of the region of interest for the input latent is large, then it will be advantageous to perform the correlation in frequency domain using fast Fourier transform (FFT) implementations where correlation reduces to multiplication, and then obtain the inverse FFT to obtain the equivalent of correlation in spatial domain.

8 Conclusions

We have proposed an OF-based registration algorithm for partial fingerprints. When we use our hierarchical registration algorithm as a pre-registration stage and reduce the search space of minutiae in the tenprint minutiae set, we were able to significantly boost the performance of two popular minutiae matchers using challenging and realistic data. The main objective of our research was to improve the rank identification accuracy for poor quality latents. We were able to obtain consistent and significant improvement for both bad and ugly quality category of latents from NIST-SD27.

On studying various OF estimation techniques for fingerprints to be used in our registration, we have noted that the best representative OF for tenprints was obtained

doi: 10.1049/iet-bmt.2014.0087

by averaging a gradient-based OF estimated from the fingerprint image and the OF reconstructed from the minutiae set. This gave the best performance mainly because of noise reduction while averaging. For latents, we studied two types of OFs corresponding to two different scenarios: with manual intervention and fully automated procedure. We obtained the best performance while using manually extracted OF for latents, and also a significant improvement with automated dictionary-based OF estimation.

We have observed that if the region of interest is very small in the latent fingerprint, especially in bad and ugly quality categories, the registration accuracy is slightly degraded while using the hierarchical method compared with correlation-based registration. This accounts for a slight variation in the Rank-1 performances between $L1$ and $L2$. Since we are not using our own minutiae matcher, but using standard ones, it will be difficult to give a theoretical justification on the behaviour for Rank-1 identification between $L1$ and $L2$, especially for bad and ugly categories. Anyway on an average, we observe that the hierarchical method significantly improves the rank identification accuracy.

We also observed that for a large quantisation step in the rotation alignment, we have not degraded the performance very much, and while matching, we have reduced the size of the minutiae search space in the tenprint to good extent which accounts for overall efficiency of our proposed method. Moreover, we have established the feasibility of our method as a fully automatic tool.

9 Acknowledgments

R.K. was supported by a Marie Curie Fellowship under project BBfor2 from European Commission (FP7-ITN-238803). This work has also been partially supported by Spanish Guardia Civil, and project Bio-Shield (TEC2012–34881) from Spanish MICINN.

10 References

1 Holder, E., Robinson, L., Laub, J.: 'The fingerprint sourcebook' (US Department of Justice, Office of Justice Programs, National Institute of Justice, Washington, DC, 2011)
2 Maltoni, D., Maio, D., Jain, A., Prabhakar, S.: 'Handbook of fingerprint recognition' (Springer Publishing Company, New York, NY, 2009)
3 Ratha, N.K., Karu, K., Chen, S., Jain, A.K.: 'A real-time matching system for large fingerprint databases', *IEEE Trans. Pattern Anal. Mach. Intell.*, 1996, **18**, (8), pp. 799–813
4 Jea, T., Govindaraju, V.: 'A minutia-based partial fingerprint recognition system', *Pattern Recognit.*, 2005, **38**, (10), pp. 1672–1684
5 Wang, Y., Hu, J.: 'Global ridge orientation modeling for partial fingerprint identification', *IEEE Trans. Pattern Anal. Mach. Intell.*, 2011, **33**, (1), pp. 72–87
6 Fang, G., Srihari, S., Srinivasan, H., Phatak, P.: 'Use of ridge points in partial fingerprint matching'. Proc. of SPIE: Biometric Technology for Human Identification IV, 2007
7 Jain, A., Chen, Y., Demirkus, M.: 'Pores and ridges: high-resolution fingerprint matching using level 3 features', *IEEE Trans. Pattern Anal. Mach. Intell.*, 2007, pp. 15–27
8 NIST: 'Evaluation of latent fingerprint technologies'. Available at http ://www.nist.gov/itl/iad/ig/latent.cfm
9 NIST: 'Summary of the results of Phase I ELFT testing'. Available at http://biometrics.nist.gov/cslinks/latent/elft07/phase1.aggregate.pdf, September 2007
10 Indovina, M., Dvornychenko, V., Tabassi, E., *et al.*: 'An evaluation of automated latent finger-print identification technology (phase II)'. Technical Report, NIST Interagency/Internal Report (NISTIR), 75-77, Apri*l* 2009
11 Indovina, M., Dvornychenko, V., *et al.*: 'Evaluation of latent fingerprint technologies: extended feature sets (evaluation 2)'. Technical Report NISTIR 7859, NIST, 2012
12 Indovina, M., Dvornychenko, V., Hicklin, R.A., *et al.*: 'NIST evaluation of latent fingerprint technologies: extended feature sets [evaluation #1]'. Technical Report, NIST Interagency/Internal Report (NISTIR), 7775, April 2011
13 Brown, L.G.: 'A survey of image registration techniques', *ACM Comput. Surv.*, 1992, **24**, (4), pp. 325–376
14 Krish, R.P., Fierrez, J., Ramos, D., *et al.*: 'Partial fingerprint registration for forensics using minutiae-generated orientation fields'. IEEE Second Int. Workshop on Biometrics and Forensics, Valletta, Malta, March 2014
15 Krish, R.P., Fierrez, J., Ramos, D., *et al.*: 'Pre-registration for improved latent fingerprint identification'. Proc. IAPR/IEEE 22nd Int. Conf. on Pattern Recognition, ICPR, Stockholm, Sweden, August 2014, pp. 696–701
16 Liu, L., Jiang, T., Yang, J., Zhu, C.: 'Fingerprint registration by maximization of mutual information', *IEEE Trans. Image Process.*, 2006, **15**, (5), pp. 1100–1110
17 Nilsson, K., Bigun, J.: 'Registration of fingerprints by complex filtering and by 1D projections of orientation images', in Kanade, T., Jain, A., Ratha, N.K., (Eds.): 'Audio-and video-based biometric person authentication' (Springer Berlin Heidelberg, 2005), pp. 171–183
18 Yager, N., Amin, A.: 'Evaluation of fingerprint orientation field registration algorithms'. Proc. Int. Conf. on Pattern Recognition (17th), 2004, vol. 4, pp. 641–644
19 Yager, N., Amin, A.: 'Fingerprint alignment using a two stage optimization', *Pattern Recognit. Lett.*, 2006, **27**, (5), pp. 317–324
20 Garris, M., McCabe, R.: 'NIST special database 27: fingerprint minutiae from latent and matching tenprint images'. Technical Report, NISTIR, 6534, 2000
21 Krish, R.P., Fierrez, J., Ramos, D., *et al.*: 'Evaluation of AFIS-ranked latent fingerprint matched template'. Sixth Pacific-Aim Symp. on Image and Video Technology, Mexico, Springer, (*LNCS*, **8333**), November 2013, pp. 230–241
22 Jain, A., Feng, J.: 'Latent fingerprint matching', *IEEE Trans. Pattern Anal. Mach. Intell.*, 2011, **33**, (1), pp. 88–100
23 Bigun, J. (ed.): 'Vision with direction: a systematic introduction to image processing and computer vision' (Springer, 2005)
24 Jiang, X., Liu, M., Kot, A.C.: 'Fingerprint retrieval for identification', *IEEE Trans. Inf. Forensics Sec.*, 2006, **1**, (4), pp. 532–542
25 Feng, J., Zhou, J., Jain, A.K.: 'Orientation field estimation for latent fingerprint enhancement', *IEEE Trans. Pattern Anal. Mach. Intell.*, 2013, **35**, (4), pp. 925–940
26 Jain, A., Feng, J.: 'Latent palmprint matching', *IEEE Trans. Pattern Anal. Mach. Intell.*, 2009, **31**, (6), pp. 1032–1047
27 Alonso-Fernandez, F., Fierrez, J., Ortega-Garcia, J., *et al.*: 'A comparative study of fingerprint image-quality estimation methods', *IEEE Trans. Inf. Forensics Sec.*, 2007, **2**, (4), pp. 734–743
28 Feng, J., Jain, A.: 'Fingerprint reconstruction: from minutiae to phase', *IEEE Trans. Pattern Anal. Mach. Intell.*, 2011, **33**, (2), pp. 209–223
29 Kass, M., Witkin, A.: 'Analyzing oriented patterns', *Comput. Vis. Graphics Image Process.*, 1987, **37**, (3), pp. 362–385
30 Available at http://www.nist.gov/itl/iad/ig/nbis.cfm (NBIS Release 4.2.0)
31 Available at http://www.biolab.csr.unibo.it (MCC SDK 1.4)
32 Cappelli, R., Ferrara, M., Maltoni, D.: 'Minutia cylinder-code: a new representation and matching technique for fingerprint recognition', *IEEE Trans. Pattern Anal. Mach. Intell.*, 2010, **32**, (12), pp. 2128–2141
33 Cappelli, R., Ferrara, M., Maltoni, D.: 'Fingerprint indexing based on minutia cylinder code', *IEEE Trans. Pattern Anal. Mach. Intell.*, 2011, **33**, (5), pp. 1051–1057
34 Ferrara, M., Maltoni, D., Cappelli, R.: 'Noninvertible minutia cylinder-code representation', *IEEE Trans. Inf. Forensics Sec.*, 2012, **7**, (6), pp. 1727–1737